Iron-meditated fungal starvation by Lupine rhizosphere-associated and extremotolerant *Streptomyces* sp. S29 desferrioxamine production

Scott A. Jarmusch[a,c]*, Diego Lagos-Susaeta[b]†, Emtinan Diab[a]†, Oriana Salazar[b], Juan A. Asenjo[b], Rainer Ebel[a], Marcel Jaspars[a]*

[a] Marine Biodiscovery Centre, Department of Chemistry, University of Aberdeen, Old Aberdeen AB24 3UE, Scotland, U.K.

[b] Centre for Biotechnology and Bioengineering, University of Chile, Beauchef 850, Santiago, Chile.

[c] Department of Medicinal Chemistry – Pharmacognosy, Uppsala University, Biomedicinskt Centrum, Uppsala, Sweden 751 23

†Authors contributed equally to this work

*Corresponding authors: scott.jarmusch@ilk.uu.se; m.jaspars@abdn.ac.uk

ABSTRACT

Siderophores are iron-chelating compounds that aid iron uptake, one of the key strategies for microorganisms to carve out ecological niches in microbially diverse environments. Desferrioxamines are the principal siderophores produced by *Streptomyces* spp. Their biosynthesis has been well studied and as a consequence, the chemical potential of the pathway continues to expand. With all of this in mind, our study aimed to explore extremotolerant and Lupine rhizosphere-derived *Streptomyces* sp. S29 for its potential antifungal capabilities. Cocultivation of isolate S29 was carried out with *Aspergillus niger* and *Botrytis cinerea*, both costly fungal phytopathogens in the wine industry. The results indicate that not only is *Streptomyces* sp. S29 extraordinary at producing hydroxamate siderophores but uses siderophore production as a means to 'starve' the fungi of iron. High resolution LC-MS/MS followed by GNPS molecular networking was used to observe the datasets for desferrioxamines and guided structure elucidation of new desferrioxamine analogues. Comparing the new chemistry, using tools like molecular networking and MS2LDA, with the known biosynthesis, we show that the chemical potential of the desferrioxamine pathway has further room for expansion.

INTRODUCTION

The application of *Streptomyces* secondary metabolites goes beyond drug discovery, as they are one of the most important bacteria for crop protection. Their biotechnological application as rhizosphere or endophytic bacteria is proven to confer protection against soilborne pathogens like fungi, nematodes, and other bacteria.[1,2] They serve as an important factor in 'disease suppressive soils', with several mechanisms of action including synthesis of plant growth regulators[3], antibiotic production[4], secretion of volatile compounds[5], and siderophore production.[6] The last of these is not only a way for bacteria to uptake vital metals from the surrounding soil but also to sequester metals in order to gain a competitive edge against other soilborne organisms.

Siderophores are iron-chelating compounds that aid metal uptake in iron deficient environments.[7] These secondary metabolites are produced by all microbes and four types of siderophore-mediated social interactions have been observed: uptake among clonal cells (sharing), cheating (which can only happen amongst microbes with the same uptake receptor), locking away, and metabolite competition (whichever microbe makes the most cost efficient and effective chelator).[8] Desferrioxamines (DFO) are the most widely observed group of siderophores in *Streptomyces* spp., used principally for Fe^{3+} scavenging[7,9], as well as some other heavy metals.[10–12] Since the vast majority of organisms require Fe^{3+} in order to maintain proper cell wall function[7], as one scavenges for itself, it simultaneously starves other competing organisms, rendering them potentially unviable.

The biosynthetic machinery of desferrioxamines has been well studied[13–15] and as a consequence, the chemical potential of the biosynthetic pathway continues to expand.

55 The substrate specificity of DesC-like proteins, similar to acyl CoA-dependent
56 transferases, seems to be the key factor in producing diverse desferrioxamine
57 scaffolds.[13,15] It has been shown that DesC can accommodate for acetyl, succinyl, and
58 myristol-CoA, with the latter providing insight into the production of acyl
59 desferrioxamines.[13] Additionally, aryl desferrioxamines, first isolated from *Micrococcus*
60 *luteus* KLE1011[16] and later from *Streptomyces sp.* MA37[17], showed further substrate
61 flexibility, where the latter communication described a new biosynthetic gene cluster
62 (BGC) which contained a DesC homolog (LgoC). This enzyme promiscuity fits ideally with
63 the Screening Hypothesis first proposed by Firn and Jones, where secondary metabolism
64 stems from metabolic pathways that 'maximize diversity and minimize cost'.[18]

65 The precursors required to drive siderophore biosynthesis have been
66 hypothesized to originate from metabolite pools (Figure 1). *Shewanella putrefaciens* has
67 been used for many of these studies, showing when precursors like putrescine are absent
68 to drive putrebactin production, lysine-based desferrioxamines are then produced.[19,20]
69 The last step in the desferrioxamine 'life-cycle' (Figure 1) is the export/import of the DFOs
70 and ferrioxamines (FOs), respectively. Import of ferrioxamines is mainly determined by
71 the protein DesE. Its role in the binding and uptake of FOs has been shown in multiple
72 studies[13,21], but most importantly, this and all other siderophore uptake mechanisms are
73 specific to their producing organisms, leading to the competition mechanisms described
74 previously.

75 Due to the modular nature of desferrioxamines and the presence of peptide bonds
76 throughout their structure, mass spectrometry-based studies have been utilized
77 extensively to not only study their biological impact but also for elucidation of new

structures. Previous studies have established standard fragmentation patterns of these siderophores, even as far as elucidating new structures solely based on mass spectrometry.[22–26] This standardized fragmentation makes the discovery of siderophores much easier thanks to metabolomics-based tools like molecular networking. Global Natural Products Social Molecular Networking (GNPS) is the most widely used platform, allowing for correlations to be drawn amongst large data sets using MS/MS.[27]

With all of this in mind, our study aimed to explore extremotolerant, rhizosphere-derived *Streptomyces* sp. S29, for its potential plant protective capabilities. Cocultivation of S29 with *Aspergillus niger* and *Botrytis cinerea*, both costly fungal phytopathogens in the wine industry, were carried out in a fashion to allow S29 to dominate the culture, thus eliciting a chemical response from the addition of each fungus. High resolution LC-MS/MS followed by GNPS molecular networking was used to analyse the data sets for desferrioxamines and guided structure elucidation of new desferrioxamines. The results of the present study indicate that not only is *Streptomyces* sp. S29 extraordinary at producing hydroxamate siderophores, totalling 16 new analogues and 9 previously identified ones confirmed through MS/MS structure elucidation, but uses siderophore production as a means to 'starve' the fungi of iron. When grown in coculture with the fungi, 9 new analogues and 16 previously described ones were identified by MS/MS. Using MS2LDA to further explore desferrioxamine chemical space, we observed that it is potentially three times larger than previously anticipated. These results point to *Streptomyces* sp. S29 being an important biocontrol agent in the plant rhizosphere.

RESULTS AND DISCUSSION

***Streptomyces* sp. S29 cocultivation and LC-MS of desferrioxamine-rich fractions.** Preliminary fungal bioassay screening of the lupine rhizosphere *Streptomyces* culture collection showed *Streptomyces* sp. S29 inhibited the growth of *Botrytis cinerea* when grown in coculture on solid medium (Figure S32). In order to induce production of potential antifungal metabolites, the bacteria and fungi were cocultivated in liquid culture in a fashion to allow for *Streptomyces* sp. to be the dominating microbe. Bioassay guided fractionation lead to no antifungal leads, yet, post-fermentation streaks showed no fungal growth (data not shown). Upon LC-MS analysis of the extracts, an abundance of DFOs was observed, leading to the hypothesis that this *Streptomyces* sp. might use a different mechanism than producing antimycotics to fight off the fungal co-cultivate, as seen previously in human bacterial infections.[28] Therefore, *Streptomyces* sp. S29 was also grown in monoculture on iron deficient medium to induce production of DFOs in an attempt to compare siderophore production to the coculture experiments. *Aspergillus niger* and *Botrytis cinerea* were chosen as the fungal phytopathogens due to their established pathology of wine producing grapes [29,30] and the importance of wine as Chile's main agricultural export, a ~ $2 billion (USD) industry.[31]

Extracts and fractions were evaluated for the presence of two DFOs (B and D1) during the fractionation steps, in order to trace the fractions that contained the highest abundance of siderophores. Presence of DFOs was further evaluated at the final stages of separation based on the molecular families generated from molecular networking, utilizing the known DFOs in the GNPS library as anchor points, which further aided structure elucidation. Based on the LC-MS results, the butanol partitions contained the

122 largest abundance of DFOs, and therefore this data was used to generate a molecular
123 network using GNPS. The standard settings of the molecular networking workflow were
124 reduced from 6 to 3 matched fragments in order to identify molecular families which
125 include closely related known DFOs. A large number of analogues found in this study did
126 not cluster into molecular families due to the varying nature of CID-MS/MS but were
127 identified manually using retention time and molecular formula comparisons.

128 **Molecular networking and MS/MS based structure elucidation.** The molecular
129 network generated contained 1208 molecular features of which 165 originated from the
130 media and instrument blanks included in the workflow. The hydroxamate siderophores
131 were distributed amongst five subnetworks (Figure 2). Closer examination of each
132 molecular family showed new analogues linking to known DFOs deposited in the GNPS
133 library. Subnetwork 1 (a1) contained a number of new acyl DFO D-like analogues that
134 are first described in this study (Figure 3). Subnetwork 2 (a2) contained various Fe^{3+} and
135 Al^{3+} complexed FOs (Figure S1). Within this network a new analogue was identified, C_{11}
136 monounsaturated acyl DFO-B, while its unbound form was not observed in culture (Figure
137 S24). Subnetworks 3 and 4 (a3 and a4) each contained one known siderophore,
138 bisucaberin-02 and legonoxamine B, respectively (Figure S2). Subnetwork 5 (a5)
139 contains one known DFO, legonoxamine A, and one additional new desferrioxamine,
140 legonoxamine E (*m/z* 537.2924, Figure S9). For the remaining nodes in a5, it was not
141 possible to assign definite structures elucidated solely based on mass spectrometry
142 (Figure S3).

143 MS/MS based structure elucidation was carried out in a similar fashion to studies
144 conducted previously (Figure 4).[22–25] Early observations of desferrioxamine B and D1

145 fragmentation showed an initial loss of the N-terminus, corresponding to the loss of either
146 118.1 or 160.1. Using this as a foundation, structures were either started with a *N*-
147 hydroxycadaverine or a *N*-hydroxy-*N*-acetylcadaverine, respectively. The remainder of
148 structure elucidation was completed stepwise: (1) predicting the molecular formula from
149 the accurate mass and collection of MS/MS data, (2) filling out the structures with the
150 typical desferrioxamine moieties of *N*-hydroxycadaverine and succinate, and (3) taking
151 the remainder of the molecular formula and placing an appropriate acid at the C-terminus
152 that either has precedent from previous studies or could be a potential binding partner
153 with an acyltransferase like coenzyme A. Overall, 25 new DFO analogues were identified
154 in the molecular network and through manual data processing (Table S1). These range
155 from short acyl chain DFO, acyl desferrioxamine D-like (DFO-D) analogues which have
156 not previously been described, aryl DFOs, and long chain dicarboxylate DFOs (Figure 5
157 and Table S1). Additionally, 25 known hydroxamate siderophores were detected,
158 including known acyl and aryl DFOs, giving further credence to the new structure
159 assignments. Their identification and observed presence in monoculture and/or coculture
160 are present in Table S1.

161 **Acyl DFO production by *Streptomyces* sp. S29.** *Streptomyces* sp. S29 was able
162 to produce seven new acyl DFOs similar to those previously described.[23,24] Of these
163 seven, five were short acyl chain derivatives (C_3, C_4, hydroxy-C_4, C_5, and C_6) and two
164 were medium monounsaturated acyl chained derivatives (C_{10} and C_{11}). The placement of
165 the alkene at the position α to the carbonyl is based off previous studies also reporting
166 DFOs containing unsaturated acyl chains.[24,32] We propose henceforth that the previously
167 known 'acyl DFOs' should be renamed 'acyl DFO-B' due to the observation in this study

168 of analogues that contain a *N*-acetyl-*N*-hydroxycadaverine terminus, similar to
169 desferrioxamine D. The new acyl DFO-D analogues discovered here also range from
170 short, medium and long acyl chained derivatives (Table S1). It is likely these acyl DFOs
171 are branched analogues as previous studies noted that it was unlikely the chains were
172 fully linear since *Streptomyces* spp. utilise branched starter units in fatty acid
173 synthesis.[23,24]

174 *Streptomyces coelicolor* has shown broad substrate specificity in regard to medium
175 and long acyl chain incorporation into desferrioxamine structures[13], but not short acyl
176 chained groups, where *Streptomyces* sp. S29 can facilitate production of short, medium,
177 and long acyl chained DFO-B analogues. Traxler et al. showed the ability of other
178 actinobacteria to react to the presence of *S. coelicolor*. through the production of acyl
179 DFO-B analogues.[23] Interestingly, we see this same phenomenon for the coculture of
180 *Streptomyces* sp. S29 and the fungi. Medium and long chained acyl DFO-Bs were almost
181 exclusively produced in coculture whereas medium and long chained acyl DFO-Ds were
182 produced under both mono- and coculture conditions. It was hypothesized these long-
183 chained derivatives might be a way for the uptake of these analogues to bypass the DesE
184 uptake mechanism, instead they 'hand-off' the Fe^{3+} via membrane bound
185 ferrioxamines.[13,33]

186 **Aryl DFO production by *Streptomyces* sp. S29.** The production of seven new
187 aryl DFOs related to legonoxamine A and B, which were also observed in this study (Table
188 S1), shows the biosynthetic flexibility of *Streptomyces* sp. S29. These structures range
189 from being smaller, potential oligomers like legonoxamine C (*m/z* 351.1912, Figure S6)
190 to the larger legonoxamine H (*m/z* 665.3893, Figure S20). Two interesting legonoxamine

191 derivatives include the putrescine-containing legonoxamine G (Figures 5B and S16) and
192 legonoxamine A glycoside (Figures 5C and S31).

193 Legonoxamine G contains a *N*-hydroxyputrescine moiety due to the initial loss of
194 104 Da instead of the typical 118 Da associated to *N*-hydroxycadaverine. Putrebactin is
195 the archetypal putrescine containing siderophore[34], and as its biosynthetic gene cluster
196 has been shown to lack genes coding for production of putrescine, it is assumed that
197 instead, this precursor is sequestered from metabolite pools.[19] Interestingly, researchers
198 have also found that under putrescine-depleted conditions, *Shewanella putrefaciens*
199 shifts to producing desferrioxamine B when cadaverine precursors are available.[35] In
200 desferrioxamine biosynthesis, incorporation of the putrescine precursor has only been
201 shown once before in desferrioxamine A[36] and now in this study with the discovery of
202 legonoxamine G.

203 Legonoxamine A glycoside was observed using the predicted molecular formula
204 ($C_{37}H_{62}N_6O_{13}$) and the loss of a sugar (-162 Da). An additional putative glycosylated DFO
205 (*m/z* 899.4827), with a predicted molecular formula of $C_{38}H_{70}N_6O_{18}$, was observed in the
206 mass spectrum but upon selected ion monitoring (SIM), produced insufficient fragment
207 ions for structural characterisation. Based on molecular formula alone, the structure of
208 this glycosylated desferrioxamine could be a C_2 acyl DFO-B diglycoside. The production
209 of glycosylated DFOs has only been reported once before: nocardamin glucuronide,
210 isolated from *Streptomyces* sp. 80H647.[37] There are only a few reports of microbial
211 enzymes that produce glucuronides[37], yet, the addition of glucose or other hexoses are
212 more commonplace in bacterial natural products.[38] We propose legonoxamine A

213 glycoside undergoes a similar glycosylation mechanism to nocardamin glucuronide,
214 occurring on a *N*-hydroxyl.

215 **Dicarboxylic acid desferrioxamine analogues.** Two new desferrioxamines,
216 observed only in coculture extracts, with dicarboxylic acid C-termini were also elucidated
217 (Figure 6A-B). Dodecanedioic DFO-B (Figure 6A and S26) has an *m/z* of 745.5086,
218 corresponding to the molecular formula of $C_{36}H_{68}N_6O_{10}$. Tridecanedioic DFO-B (Figure
219 6B and S28) has an *m/z* of 759.5221, corresponding to the molecular formula of
220 $C_{37}H_{70}N_6O_{10}$. This is the first reported instance of dicarboxylic acids larger than succinate
221 being incorporated into DFO structures yet there are examples of larger dicarboxylic acids
222 being bound to CoA, like pimelic acid, therefore we cannot rule the possibility out. Based
223 on formula predictions and the lack of further fragmentation, the proposed structures are
224 based on the biosynthesis and the mass spectrometric data obtained. Further
225 investigation into these dicarboxylic acid products is currently underway.

226 **Ferrioxamines and DFO presence in pure and coculture experiments.** A
227 number of metal complexed ferrioxamines were observed in subnetwork 2 (Figure S1).
228 Fe^{3+} and Al^{3+} are the only metals complexed with the variety of desferrioxamines present,
229 similar to studies before (Figure S1).[24,26] The binding efficiencies for Fe^{3+} and Al^{3+} are
230 similar, therefore there seems to be no overwhelming preference for either.[39] The
231 importance of iron has already been addressed in regard to bacteria and cell maintenance
232 but Al^{3+} is toxic and has no direct role in metabolism and seems to be an unintended
233 biological activity of these metabolites.

234 The molecular network was also used to evaluate the production of the DFOs
235 between the two cocultivations with *A. niger* and *B. cinerea* and the *Streptomyces* sp.

236 S29 monoculture. The results showed that 25 of the 50 were present in the monoculture,
237 whereas all of the remaining were found in coculture extracts only (Table S1). There was
238 no significant difference in the siderophores produced under cocultivation with *A. niger* or
239 *B. cinerea*, indicating the potential broad response to a fungal microbe in the environment.
240 This result might point to DFO and siderophore production as a common chemical
241 response to other microbes, whether it be bacterial or fungal, in close environmental
242 proximity to the primary organism.

243 **MS2LDA analysis.** In order to further evaluate the overall chemical space that
244 DFOs inhabit in the molecular network, MS2LDA was performed. MS2LDA is a technique
245 which identifies molecular 'fingerprints' in fragmentation patterns and assigns these into
246 motifs (13 Mass2Motifs were manually curated). By merging the two networks (GNPS
247 molecular network and MS2LDA) after motifs were annotated, it is clear that further DFO
248 chemical space is there to be discovered. Figure S4 represents the overall results of this
249 merged network where 4A highlights the previously identified nodes (55) and edges (573)
250 from the original molecular networking job and 4B highlights all of the nodes (147) and
251 edges (1158) that contain DFO motifs identified through MS2LDA. This tripling of nodes
252 by inclusion of the MS2LDA workflow shows a clear expansion of DFO chemical space
253 that other studies up to this date have yet been able to show.

254 In order to evaluate the accuracy of this analysis, a characterized DOF in this study
255 (legonoxamine E, Figure 5A) and an unknown DFO observed using MS2LDA (*m/z*
256 650.37, $[M+2H]^{2+}$) were more closely analysed (Figure S5). The unknown
257 desferrioxamine is a singleton (Figure S5B) in both the original network and the merged
258 network, yet, MS2LDA identifies it contains DFO motifs and upon closer inspection and

259 prediction of its molecular formula ($C_{59}H_{103}N_{12}O_{20}$), it seems to be a novel dodecadentate
260 DFO, which would point to it being able to bind two moles of Fe^{3+}. Elucidation of its full
261 structure was not able to be completed with MS/MS data alone, therefore, further studies
262 are required to characterise its structure.

263 ***Streptomyces* sp. S29 siderophore biosynthetic gene clusters.** DFOs are
264 biosynthesized by nonribosomal peptide synthetase independent siderophore (NIS)
265 pathways and the presence of at least one gene encoding a homolog to IucA/IucC has
266 become recognized as a marker of NIS BGCs.[40,41] DFO biosynthesis is encoded by the
267 highly conserved *des* BGC (*desEFABCD* genes) found in many *Streptomyces* species [42].
268 Using FeGenie[43], the identification of iron-related genes revealed 27 siderophore
269 biosynthesis and 11 transport related genes in the *Streptomyces* sp. S29 genome. These
270 siderophore biosynthesis related genes are grouped in five biosynthetic gene clusters
271 and antiSMASH [44] predictions reveal that three of the five contain at least one gene
272 homolog to IucA/IucC and the other two correspond to NRPS dependent pathways. In *S.*
273 *coelicolor* A3(2), transcription of *des* BGC is repressed by the divalent metal-dependent
274 regulatory (DmdR) protein DmdR1 and derepressed by iron limitation.[45] BLASTN/P
275 analysis revealed a putative DmdR repressor in *Streptomyces* sp. S29 (s29_002782) with
276 89% nucleotide and 93% amino acid identity to DmdR1 (AJ271797.1 / CAC28070.1).
277 BLASTN analyses identified eight putative DmdR-binding sites (iron boxes) in
278 *Streptomyces* sp. S29 by query of putative iron boxes found upstream in different ORFs
279 in *S. coelicolor* A3(2) genome.[13]

280 The three NIS BGCs (Figure S31A-C) were all independently evaluated against
281 the two known desferrioxamine BGCs. All three ORFs are present in numerous

282 *Streptomyces* spp. yet based on the biosynthetic genes, only those found in regions 7
283 and 9 of the antiSMASH analysis are potentially related to *des*. Region 7 (Figure S31A)
284 contains a siderophore BGC in *Streptomyces* sp. S29 with high homology to *desA-D*
285 genes and to the ferric-siderophore uptake and utilization genes (*desE-F*). This *des*
286 cluster follows the same structure as many *Streptomyces* spp., including the position of
287 iron boxes upstream putative *desE* (s29_002291) and *desA* (s29_002293) genes (Fig
288 S31). DesC of the *des* BGC from *Streptomyces* sp. S29 (s29_2295) exhibits high identity
289 to DesC from S. coelicolor (72%) and to LgoC from *Streptomyces* sp. MA37 (69%).
290 Regions 9 and 14 are each siderophore BGCs but the gene clusters and its products are
291 uncharacterized and unknown. Region 9 (Figure S31B) comprises the essential genes
292 required to be a NIS BGC related to *des*, like an iron transporter, a IucA/IucC family
293 siderophore biosynthesis protein and an acyltransferase (s29_4785) with moderate
294 homology to DesC (30%) and LgoC (32%). Region 14 (Figure S31C) lacks an
295 acyltransferase which points to this gene cluster not being related to *des*.

296 Acyltransferases involved in hydroxamate biosynthesis normally exhibit narrow
297 substrate tolerance (e.g. IucB, which shows a high degree of specificity towards acetyl-
298 CoA).[13] The array of DFOs produced by *S. coelicolor* (B, E, G1 and amphiphilic) and aryl
299 DFOs (legonoxamine A-B) produced by *Streptomyces* sp. MA37, has been attributed to
300 substrate tolerant acyltransferases DesC and LgoC. [13,46] Senges et al. acknowledged in
301 their evaluation of the *Streptomyces chartreusis* secretome that in iron depleted minimal
302 medium they also observed additional desferrioxamines produced and that the overall
303 biosynthetic potential may be much broader than what has been predicted.[25] While the
304 biosynthesis of the *des* gene cluster in *Streptomyces* sp. S29 needs further studying, the

305 chemical potential shown in this study highlights its ability for producing a wide range of
306 DFOs.

307 In conclusion, the chemistry observed in the *Streptomyces* sp. S29 secretome
308 shows it potential as an agent to prevent fungal infection, evidenced in the overproduction
309 of desferrioxamines observed via mass spectrometry. New analogues were observed in
310 both monoculture and cocultivation studies with fungal phytopathogens, *A. niger* and *B.*
311 *cinerea*. *Streptomyces* sp. S29 seems to produce an arsenal of desferrioxamine
312 analogues using any available precursor materials available whether that be putrescine,
313 cadaverine, aryl, acyl, or long chained dicarboxylates. The role of bacterial communities
314 in plant and crop protection is becoming more important due to the growing world
315 population, with a strong emphasis on improving strategies at preventing phytopathogenic
316 infection. Overall, the production of 25 new and 25 previously reported siderophores
317 indicates this *Streptomyces* sp. should be studied further for its plant protective properties
318 as a biocontrol agent.

319

320 **EXPERIMENTAL SECTION**

321 *Strain collection*

322 *Streptomyces* sp. S29 was isolated from a soil sample collected from Lupine plant
323 (*Lupinus oreophilus*) roots originating from a polyextreme enviroment at Quebrada
324 Nacimiento, Socaire, San Pedro de Atacama, Atacama desert (Northern Chile)
325 [23°37’06’’S;67°50’56’’W - 3,646 m.a.s.l]. One aliquot was heated at 100 [°C] for 5 [min]
326 and directly sprinkled onto Gause #1 and Starch-Casein plates, both complemented with

327 Nystatin, Cycloheximide and Nalidixic acid. Another aliquot was resuspended in 1⁄4
328 Ringer solution, heated at 60 [°C] for 10 [min] and dilutions of $10^{-1/2}$ and 10^{-1} were spread
329 onto agar plates. Plates were incubated at 30 [°C] for ~1 week and colonies were
330 subcultured on ISP2 plates. Based on morphological characteristics of the colony and
331 antifungal activity experiments against *B. cinerea* and *A. niger*, 16S rRNA sequence of
332 S29 isolate was used to identify and confirm its taxonomy using EzBioCloud database (3)
333 (data not shown).
334
335 *Phytopathogens*
336 *Aspergillus niger* and *Botrytis cinerea*, biochemically characterized field samples, were
337 provided by Laboratorio de microbiología, Facultad de Ciencias naturales, matemática y
338 medio ambiente, Universidad Tecnológica Metropolitana (UTEM), Santiago, Chile.
339 Molecular identification of these strains was carried out by sequencing of internal
340 transcribed spacer (ITS) region amplified by PCR using universal primers ITS1 and ITS4
341 (supplementary data).
342

343 *Streptomyces sp. S29 genome sequencing and assembly*

344 *Streptomyces* sp. S29 total DNA was extracted from liquid culture using DNeasy
345 UltraClean Microbial Kit (Qiagen). Whole genome sequencing (WGS) of the strain was
346 performed by an Illumina MiSeq (2 x 300 PE). Nanopore sequencing was performed using
347 a Rapid Sequencing Kit (SQK-RAD004) and MinIon Flow Cell (R9.4.1). The sequence
348 was assembled using Canu, polished using Racon, Illumina dataset was mapped onto
349 the contigs using BWA mem and then corrected using Pilon. The genome was annotated

350 using NCBI pgap software (6). Raw reads from short-read (Illumina) and long-read
351 (Nanopore) sequencing were deposited in the NCBI Sequence Read Archive (SRA): SRA
352 accession number XXXXX. Complete genome sequences were deposited in GenBank
353 via the NCBI's submission portal: Genome accession number XXXXX.

354 *Cocultivation and extraction*

355 A set of experiments were carried out on these three organisms in order to determine the
356 effect of the fungal culture being added to the *Streptomyces* sp. (a) *Streptomyces* sp. S29
357 alone: a single colony was aseptically transferred to 100 mL of iron deficient medium
358 (ISP2) in order to induce production of siderophores and was fermented for 7 days. (b)
359 *Streptomyces* sp. S29 + *Aspergillus niger*: 100 mL of bacterial culture was grown for 5
360 days. Simultaneously, an independent axenic culture of *A. niger* was grown for 3 days
361 (10 mL of PDA liquid medium). On the fifth day, the fungal culture was transferred
362 aseptically to the bacterial culture and allowed to grow an addition 2 days. (c)
363 *Streptomyces* sp. S29 + *Botrytis cinerea*: the same procedure as described in experiment
364 b was followed.

365 Each liquid fermentation included Diaion HP-20 resin (3 g/50 mL) that was
366 sterilised with culture medium. After 7 days, the resin was vacuum filtered, subsequently
367 washed five times with milli-q water and finally macerated exhaustively in methanol (3×).
368 The methanolic extract was then dried on a rotary evaporator and subsequently
369 underwent Kupchan partitioning.[47] Finally, the *sec*-butanol fraction underwent C18 solid-
370 phase extraction (Phenomenex), with each separation yielding 5 fractions of increasing
371 methanol and these samples were subsequently prepared for LC-MS studies.

372 The 100% methanol fractions from the *Botrytis* and *Aspergillus* co-culture were
373 subjected to further separation via reversed phase-HPLC with a Waters Sunfire C18
374 semi-preparative column (5 μM, 100Å, 250 × 10 mm) wand a solvent system of A–95/5
375 MeOH/H_2O and B-MeOH. The Agilent 1200 HPLC utilized a solvent gradient of 0% B to
376 100% B at 2.0 mL/min over 50 min.

377 *Liquid chromatography – mass spectrometry*

378 All runs were analysed using an Agilent 1290 UHPLC coupled to Bruker MAXIS II Q-ToF
379 mass spectrometer. LC utilizes a Phenomenex Kinetex XB-C_{18} (2.6 mM, 100 × 2.1 mm)
380 column with a mobile phase of 5% MeCN+0.1% formic acid to 100% MeCN+0.1% formic
381 acid in 11 min. Bruker MAXIS II has a mass range of *m/z* 100-2000, capillary voltage 4.5
382 kV, nebulizer gas 5.0 bar, dry gas 12.0 l/min, and dry temperature of 220 °C. MS/MS
383 experiments were conducted under Auto MS/MS scan mode with a step collision energy
384 from 80-200%. Samples were prepared at a concentration of 0.3 mg/mL. Raw data files
385 were analysed using Bruker Daltonics 3.6.
386

387 *GNPS Molecular Networking and MS2LDA*

388 A molecular network was created using the online workflow (https://ccms-
389 ucsd.github.io/GNPSDocumentation/) on the GNPS website (http://gnps.ucsd.edu).[27]
390 The data was filtered by removing all MS/MS fragment ions within ± 17 Da of the precursor
391 *m/z*. MS/MS spectra were window filtered by choosing only the top 6 fragment ions in the
392 ± 50 Da window throughout the spectrum. The precursor ion mass tolerance was set to
393 2.0 Da and a MS/MS fragment ion tolerance of 0.5 Da. A network was then created where

394 edges were filtered to have a cosine score above 0.7 and more than 3 matched peaks.
395 Further, edges between two nodes were kept in the network if and only if each of the
396 nodes appeared in each other's respective top 10 most similar nodes. Finally, the
397 maximum size of a molecular family was set to 0, and the lowest scoring edges were
398 removed from molecular families until the molecular family size was below this threshold.
399 The spectra in the network were then searched against GNPS' spectral libraries. The
400 library spectra were filtered in the same manner as the input data. All matches kept
401 between network spectra and library spectra were required to have a score above 0.7
402 and at least 6 matched peaks.
403
404 For documentation on running MS2LDA, the user is referred to the original publication
405 and guidelines, which are also present at ms2lda.org.[48] All spectral images in the
406 supplementary information were created using Metabolomics Spectrum Resolver
407 (https://metabolomics-usi.ucsd.edu/).[49]
408 All siderophores dereplicated and elucidated in this study can be found in Table
409 S1. The structure elucidation of each new derivative and its corresponding MS/MS
410 spectra were generated using Metabolomics Spectrum Resolver are displayed in the
411 supplementary information (Table S2 and Figures S6-S31). All MS/MS spectra were also
412 annotated and deposited in the GNPS library, as well as the original datasets (Table S2).
413
414 **ASSOCIATED CONTENT**
415 **Supplementary Information**

Tables of known and new desferrioxamine derivatives (Table S1) and their corresponding CCMS Library IDs and Metabolomics Resolver Images (Table S2), Desferrioxamine containing subnetworks, new desferrioxamine analogues with annotated structures and MS^2 spectra, preliminary fungal bioassay image, ITS regions for fungal phytopathogens.

Author Contributions

DLS† and ED† contributed equally to this work.

Acknowledgements

SAJ would like to thank the University of Aberdeen for funding doctoral studies through and Elphinstone Scholarship. DL would like to thank the Agencia Nacional de Investigación y Desarrollo [ANID] for funding doctoral studies through 'Beca nacional de doctorado' Scholarship. ED would like to thank the Ministry of Higher Education and Scientific Research - Sudan, together with the University of Khartoum, for joint funding of masters studies. We would like to thank to Valeria Razmilic and Jean Franco Castro for their valuable advice and work in the setup of Lupine *Streptomyces* culture collection. We would also like to thank the support team at GNPS and Justin J.J. van der Hooft at MS2LDA for help with data deposition and for help at any stage of running the relevant workflows.

References

1 R. G. Expósito, I. de Bruijn, J. Postma and J. M. Raaijmakers, *Frontiers in Microbiology*, 2017, 8.

2 O. S. Olanrewaju and O. O. Babalola, *Applied Microbiology and Biotechnology*, 2019, 103, 1179–1188.

3 Y. Goudjal, O. Toumatia, N. Sabaou, M. Barakate, F. Mathieu and A. Zitouni, *World Journal of Microbiology and Biotechnology*, 2013, **29**, 1821–1829.

4 O. S. Olanrewaju and O. O. Babalola, *Applied Microbiology and Biotechnology*, 2019, 103, 1179–1188.

5 S. E. Jones and M. A. Elliot, *Trends in Microbiology*, 2017, 25, 522–531.

6 V. C. Verma, S. K. Singh and S. Prakash, *Journal of Basic Microbiology*, 2011, **51**, 550–556.

7 M. Sandy and A. Butler, *Chemical Reviews*, 2009, **109**, 4580–4595.

8 J. Kramer, Ö. Özkaya and R. Kümmerli, *Nature Reviews Microbiology*, 2020, 18, 152–163.

9 R. Saha, N. Saha, R. S. Donofrio and L. L. Bestervelt, *Journal of Basic Microbiology*, 2013, **53**, 303–317.

10 B. Casentini and M. Pettine, *Applied Geochemistry*, 2010, **25**, 1688–1698.

11 K. E. Jones, K. L. Batchler, C. Zalouk and A. M. Valentine, *Inorganic Chemistry*, 2017, **56**, 1264–1272.

12 U. Neubauer, G. Furrer and R. Schulin, *European Journal of Soil Science*, 2002, **53**, 45–55.

13 J. L. Ronan, N. Kadi, S. A. McMahon, J. H. Naismith, L. M. Alkhalaf and G. L. Challis, *Philosophical Transactions of the Royal Society B: Biological Sciences*, , DOI:10.1098/rstb.2017.0068.

14 T. Schupp, U. Waldmeier and M. Divers, *FEMS Microbiology Letters*, 1987, **42**, 135–139.

15 F. Barona-Gómez, U. Wong, A. E. Giannakopulos, P. J. Derrick and G. L. Challis, *Journal of the American Chemical Society*, 2004, **126**, 16282–16283.

16 A. D'Onofrio, J. M. Crawford, E. J. Stewart, K. Witt, E. Gavrish, S. Epstein, J. Clardy and K. Lewis, *Chemistry and Biology*, 2010, **17**, 254–264.

17 F. Maglangit, M. H. Tong, M. Jaspars, K. Kyeremeh and H. Deng, *Tetrahedron Letters*, 2019, **60**, 75–79.

18 R. D. Firn and C. G. Jones, *Natural Product Reports*, 2003, 20, 382–391.

19 S. Rütschlin, S. Gunesch and T. Böttcher, *Cell Chemical Biology*, 2017, **24**, 598-604.e10.

20 C. Z. Soe, A. A. H. Pakchung and R. Codd, *Chemistry & Biodiversity*, 2012, **9**, 1880–1890.

21 V. H. Tierrafría, H. E. Ramos-Aboites, G. Gosset and F. Barona-Gómez, *Microbial Biotechnology*, 2011, **4**, 275–285.

22 T. Pluháček, K. Lemr, D. Ghosh, D. Milde, J. Novák and V. Havlíček, *Mass Spectrometry Reviews*, 2016, **35**, 35–47.

23 M. F. Traxler, J. D. Watrous, T. Alexandrov, P. C. Dorrestein and R. Kolter, *mBio*, , DOI:10.1128/mBio.00459-13.

24 A. M. Sidebottom, A. R. Johnson, J. A. Karty, D. J. Trader and E. E. Carlson, *ACS Chemical Biology*, 2013, **8**, 2009–2016.

25 C. H. R. Senges, A. Al-Dilaimi, D. H. Marchbank, D. Wibberg, A. Winkler, B. Haltli, M. Nowrousian, J. Kalinowski, R. G. Kerr and J. E. Bandow, *Proceedings of the National Academy of Sciences of the United States of America*, 2018, **115**, 2490–2495.

26 W. J. Moree, V. v. Phelan, C. H. Wu, N. Bandeira, D. S. Cornett, B. M. Duggan and P. C. Dorrestein, *Proceedings of the National Academy of Sciences of the United States of America*, 2012, **109**, 13811–13816.

27 M. Wang, J. J. Carver, V. v. Phelan, L. M. Sanchez, N. Garg, Y. Peng, D. D. Nguyen, J. Watrous, C. A. Kapono, T. Luzzatto-Knaan, C. Porto, A. Bouslimani, A. v. Melnik, M. J. Meehan, W. T. Liu, M. Crüsemann, P. D. Boudreau, E. Esquenazi, M. Sandoval-Calderón, R. D. Kersten, L. A. Pace, R. A. Quinn, K. R. Duncan, C. C. Hsu, D. J. Floros, R. G. Gavilan, K. Kleigrewe, T. Northen, R. J. Dutton, D. Parrot, E. E. Carlson, B. Aigle, C. F. Michelsen, L. Jelsbak, C. Sohlenkamp, P. Pevzner, A. Edlund, J. McLean, J. Piel, B. T. Murphy, L. Gerwick, C. C. Liaw, Y. L. Yang, H. U. Humpf, M. Maansson, R. A. Keyzers, A. C. Sims, A. R. Johnson, A. M. Sidebottom, B. E. Sedio, A. Klitgaard, C. B. Larson, C. A. P. Boya, D. Torres-Mendoza, D. J. Gonzalez, D. B. Silva, L. M. Marques, D. P. Demarque, E. Pociute, E. C. O'Neill, E. Briand, E. J. N. Helfrich, E. A. Granatosky, E. Glukhov, F. Ryffel, H. Houson, H. Mohimani, J. J. Kharbush, Y. Zeng, J. A. Vorholt, K. L. Kurita, P. Charusanti, K. L. McPhail, K. F. Nielsen, L. Vuong, M. Elfeki, M. F. Traxler, N. Engene, N. Koyama, O. B. Vining, R. Baric, R. R. Silva, S. J. Mascuch, S. Tomasi, S. Jenkins, V. Macherla, T. Hoffman, V. Agarwal, P. G. Williams, J. Dai, R. Neupane, J. Gurr, A. M. C. Rodríguez, A. Lamsa, C. Zhang, K. Dorrestein, B. M. Duggan, J. Almaliti, P. M. Allard, P. Phapale, L. F. Nothias, T. Alexandrov, M. Litaudon, J. L. Wolfender, J. E. Kyle, T. O. Metz, T. Peryea, D. T. Nguyen, D. VanLeer, P. Shinn, A. Jadhav, R. Müller, K. M. Waters, W. Shi, X. Liu, L. Zhang, R. Knight, P. R. Jensen, B. Palsson, K. Pogliano, R. G. Linington, M. Gutiérrez, N. P. Lopes, W. H. Gerwick, B. S. Moore, P. C. Dorrestein and N. Bandeira, *Nature Biotechnology*, 2016, 34, 828–837.

28 B. D. Corbin, E. H. Seeley, A. Raab, J. Feldmann, M. R. Miller, V. J. Torres, K. L. Anderson, B. M. Dattilo, P. M. Dunman, R. Gerads, R. M. Caprioli, W. Nacken, W. J. Chazin and E. P. Skaar, *Science*, 2008, **319**, 962–965.

29 P. A. G. Elmer and T. Reglinski, *Plant Pathology*, 2006, 55, 155–177.

30 G. Perrone, A. Susca, G. Cozzi, K. Ehrlich, J. Varga, J. C. Frisvad, M. Meijer, P. Noonim, W. Mahakamchanakul and R. A. Samson, in *Studies in Mycology*, Centraalbureau voor Schimmelculturen, 2007, vol. 59, pp. 53–66.

31 ODEPA - Oficina de Estudios y Políticas Agrarias, Vinos, https://www.odepa.gob.cl/rubros/vinos-y-alcoholes, (accessed May 26, 2020).

32 M. Luo, E. A. Fadeev and J. T. Groves, *Journal of the American Chemical Society*, 2005, **127**, 1726–1736.

33 J. S. Martinez, G. P. Zhang, P. D. Holt, H. T. Jung, C. J. Carrano, M. G. Haygood and A. Butler, *Science*, 2000, **287**, 1245–1247.

34 K. M. Ledyard, A. Butler, K. M. Ledyard and A. Butler, *Structure of putrebactin, a new dihydroxamate siderophore produced by Shewanella putrefaciens*, 1997, vol. 2.

35 C. Z. Soe, A. A. H. Pakchung and R. Codd, *Directing the Biosynthesis of Putrebactin or Desferrioxamine B in Shewanella putrefaciens through the Upstream Inhibition of Ornithine Decarboxylase*, .

36 W. Keller-Schierlein, P. Mertens, V. Prelog and A. Walser, *Helvetica Chimica Acta*, 1965, **48**, 710–723.

37 J. A. v. Lopez, T. Nogawa, Y. Futamura, T. Shimizu and H. Osada, *Journal of Antibiotics*, 2019, **72**, 991–995.

38 S. I. Elshahawi, K. A. Shaaban, M. K. Kharel and J. S. Thorson, *Chemical Society Reviews*, 2015, 44, 7591–7697.

39 T. C. Johnstone and E. M. Nolan, *Dalton Transactions*, 2015, 44, 6320–6339.

40 G. L. Challis, *ChemBioChem*, 2005, 6, 601–611.

41 N. Kadi and G. L. Challis, *Methods in Enzymology*, 2009, 458, 431–457.

42 F. Barona-Gómez, S. Lautru, F. Francois-Xavier, P. Leblond, J. L. Pernodet and G. L. Challis, *Microbiology*, 2006, **152**, 3355–3366.

43 A. I. Garber, K. H. Nealson, A. Okamoto, S. M. McAllister, C. S. Chan, R. A. Barco and N. Merino, *Frontiers in Microbiology*, 2020, **11**, 37.

44 K. Blin, S. Shaw, K. Steinke, R. Villebro, N. Ziemert, S. Y. Lee, M. H. Medema and T. Weber, *Nucleic acids research*, 2019, **47**, W81–W87.

45 F. J. Flores and J. F. Martín, *Biochemical Journal*, 2004, **380**, 497–503.

46 F. M. Maglangit, S. Alrashdi, J. Renault, L. Trembleau, C. Victoria, M. H. Tong, S. Wang, K. Kyeremeh and H. Deng, *Organic & Biomolecular Chemistry*, , DOI:10.1039/D0OB00320D.

47 W. Houssen and M. Jaspars, in *Natural Products Isolation*, ed. A. Sarker, S.; Latfi, Z.; Gray, Humana Press, Second., 2006, p. 380.

48 J. J. J. van der Hooft, J. Wandy, M. P. Barrett, K. E. V. Burgess and S. Rogers, *Proceedings of the National Academy of Sciences of the United States of America*, 2016, **113**, 13738–13743.

49 M. Wang, S. Rogers, W. Bittremieux, C. Chen, P. C. Dorrestein, E. L. Schymanski, T. Schulze, S. Neumann and R. Meier, *bioRxiv*, 2020, 2020.05.09.086066.

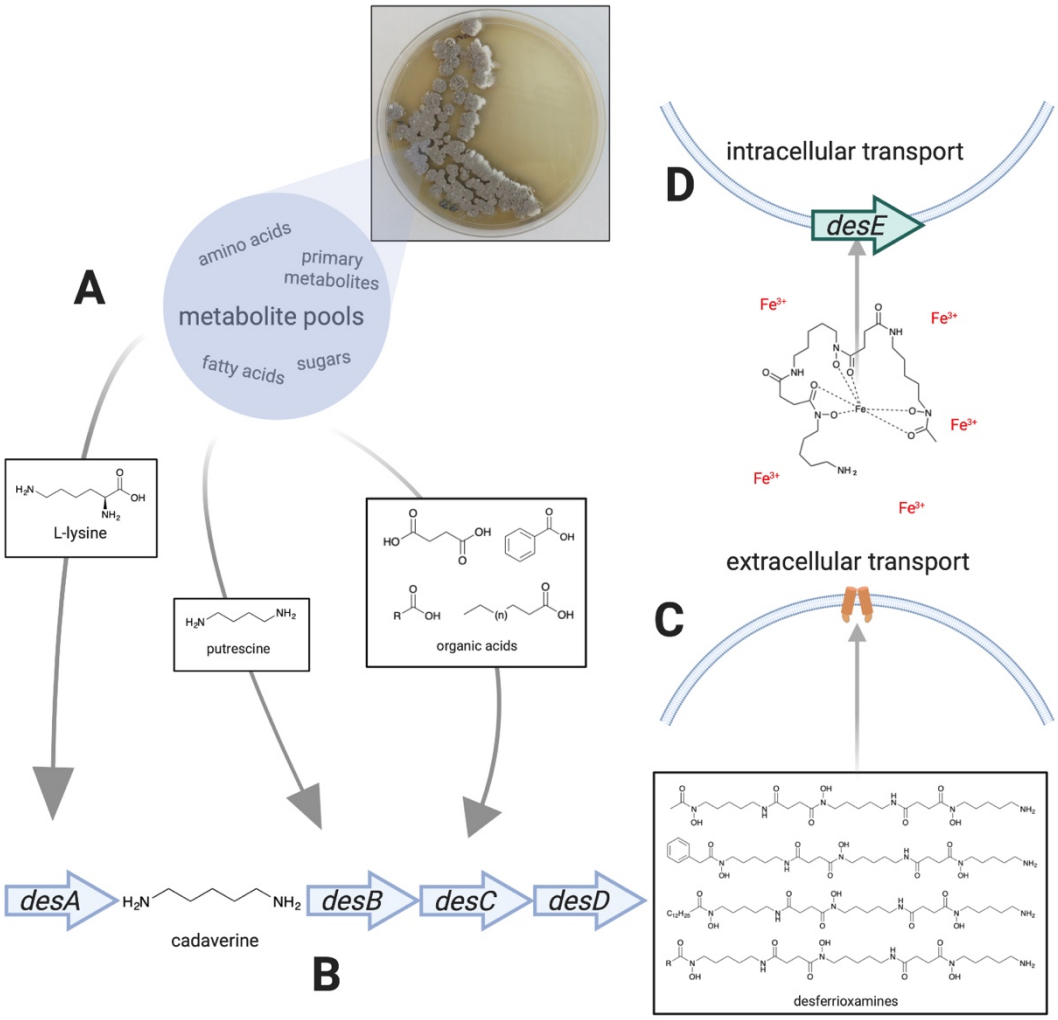

Figure 1. Desferrioxamine 'life-cycle'. (A) metabolite pools are generated in the bacterium, allowing for resources to be feed into the biosynthetic machinery. (B) desferrioxamine biosynthesis is dictated by the presence or absence of the proper precursors in the metabolite pools. The substrate flexibility of DesC allows for precursor organic acids to be integrated into a wide variety of structures. (C) the mature desferrioxamines are then transported into the extracellular environment to sequester Fe3+ and finally, (D), the iron-bound ferrioxamine

metabolites are then imported via specified uptake mechanisms (desE or other membrane bound mechanisms). Created with BioRender.com.

557

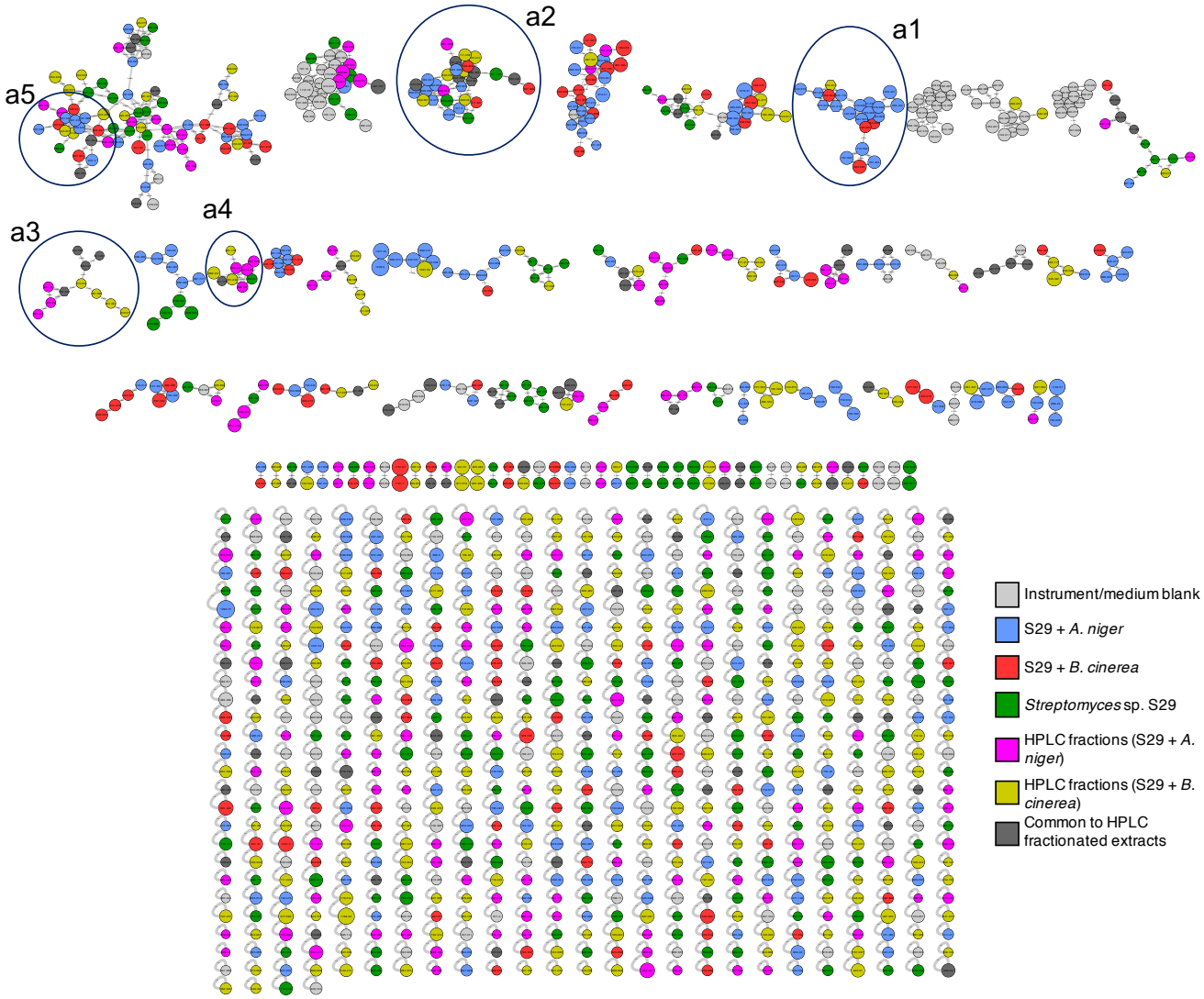

Figure 2. Molecular network containing all sec-butanol SPE fractions from monocultures, cocultures, and instrument and medium blanks. Node size represents *m/z* of each molecular feature. Nodes are connected if the cosine score meets the threshold set in the molecular networking workflow (≥0.7) and if the minimum amount of matched fragment peaks is met (minimum of 3). Circled molecular families represent those containing desferrioxamines.

558

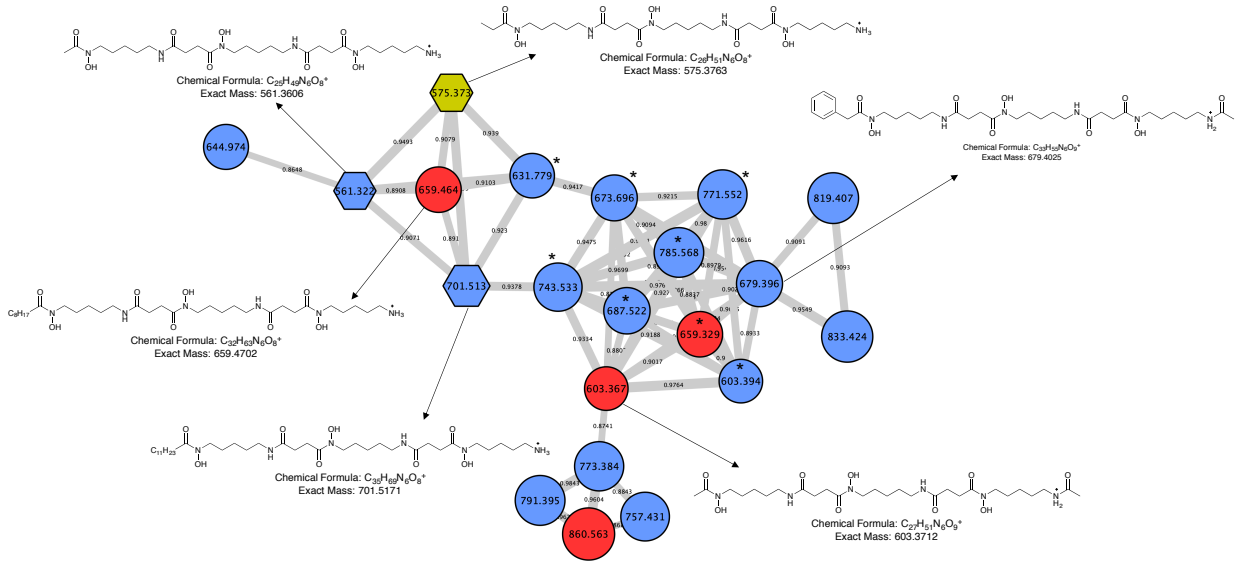

Figure 3. Desferrioxamine subnetwork 1. Desferrioxamine B (561.322), desf-05 (575.375), and C_{11} acyl DFO (701.513) were identified (represented as hexagons). Desferrioxamine D1 (603.367) and acyl ferrioxamine 1/legonoxamine A (679.396) were also identified through fragmentation comparison. All features with * represent new desferrioxamines identified through MS/MS fragmentation pattern analysis.

559

560

561

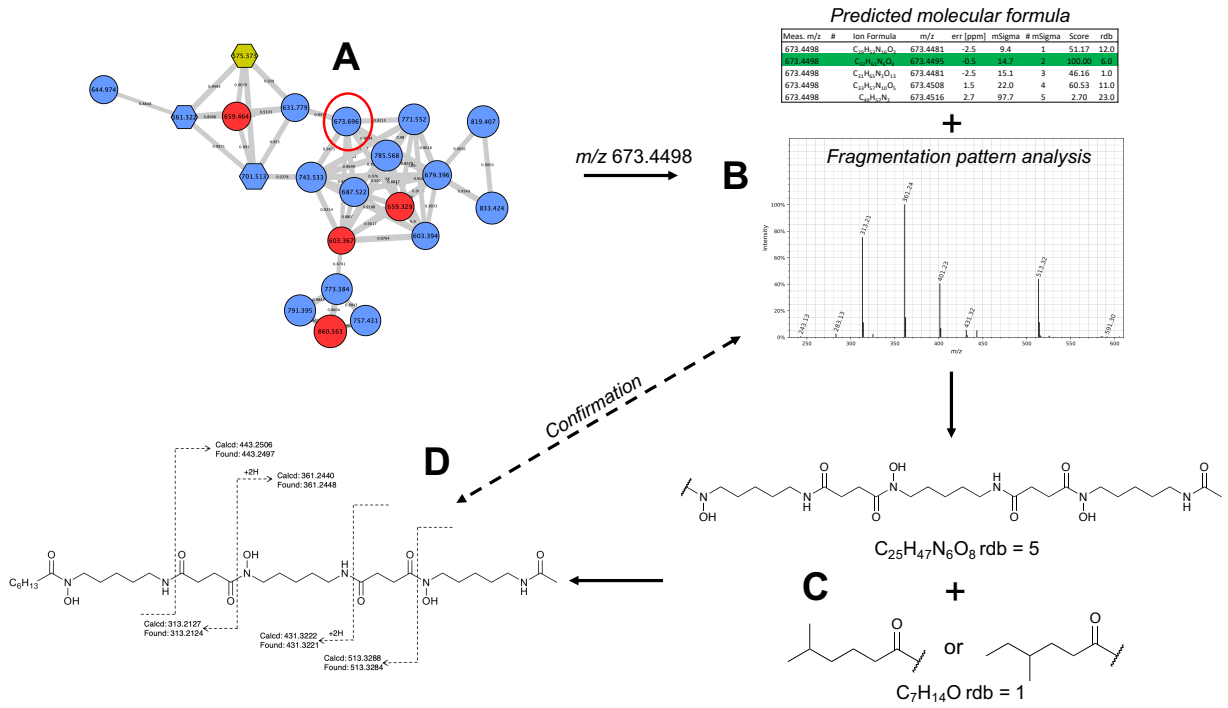

Figure 4. Molecular network and MS/MS based structure determination. (A) molecular networks generated using GNPS were dereplicated and potentially unknown ions were found in the Raw data. (B) Predicted molecular formula were generated and the most likely candidate formula was chosen. MS/MS spectra were analysed for the initial loss of -118 or -160 to determine the N-terminal moiety of *N*-hydroxycadaverine or *N*-acetylhydroxycadaverine, respectively. (C) Based on known structure of desferrioxamines, substructures were proposed for each new metabolite and lastly, (D) putative structures were confirmed using the MS/MS data.

562

563

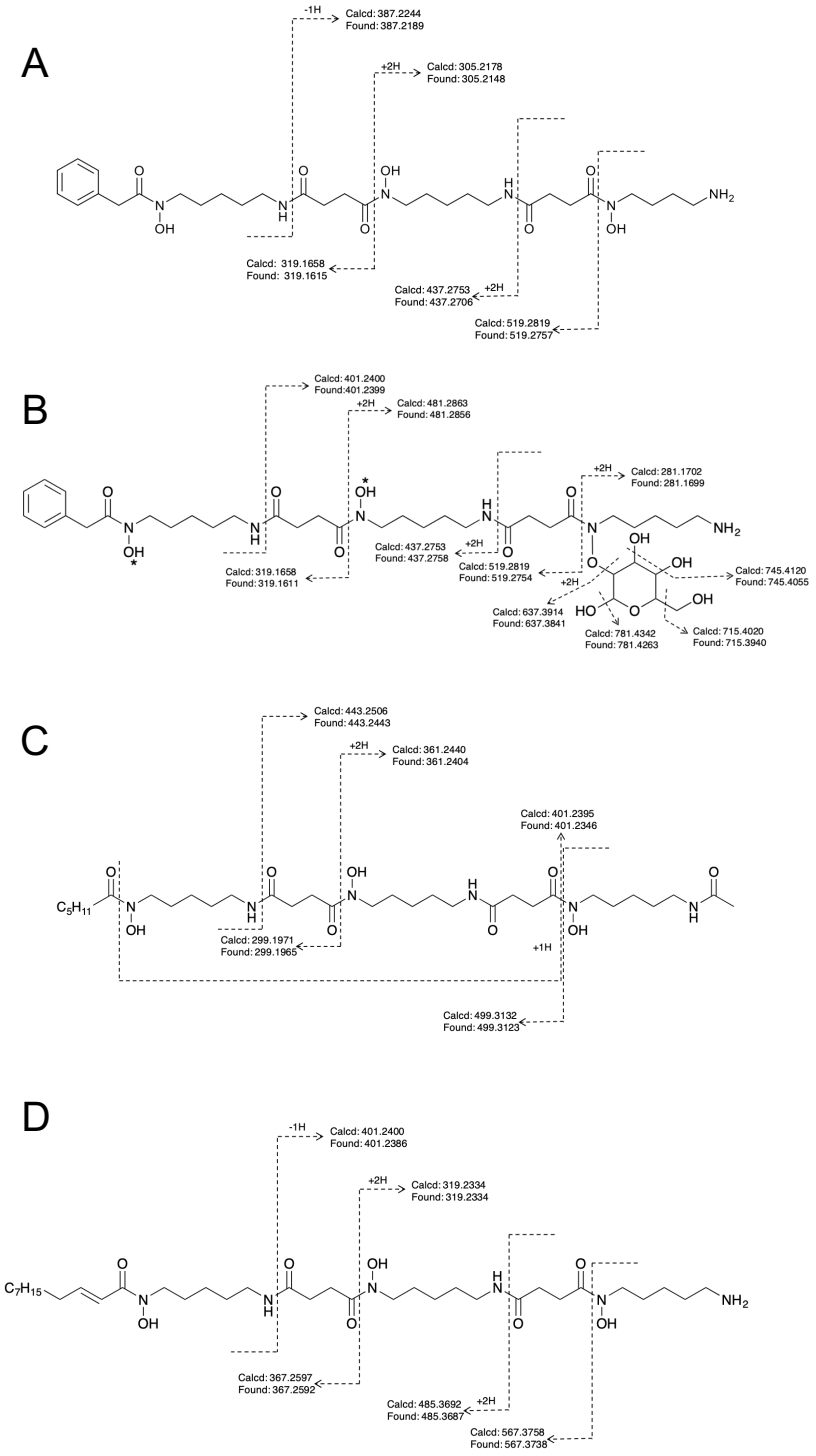

Figure 5. Representation of desferrioxamine structural diversity of *Streptomyces* sp. S29. (A-B) New legonoxamine derivatives were some of the most abundant

desferrioxamines present in the culture, represented here by legonoxamine G (contains N-terminal *N*-hydroxyputrescine) and legonoxamine A glycoside, respectively. (C-D) New acyl DFOs were also observed, including acyl DFO-Ds and monounsaturated acyl DFO-Bs.

564

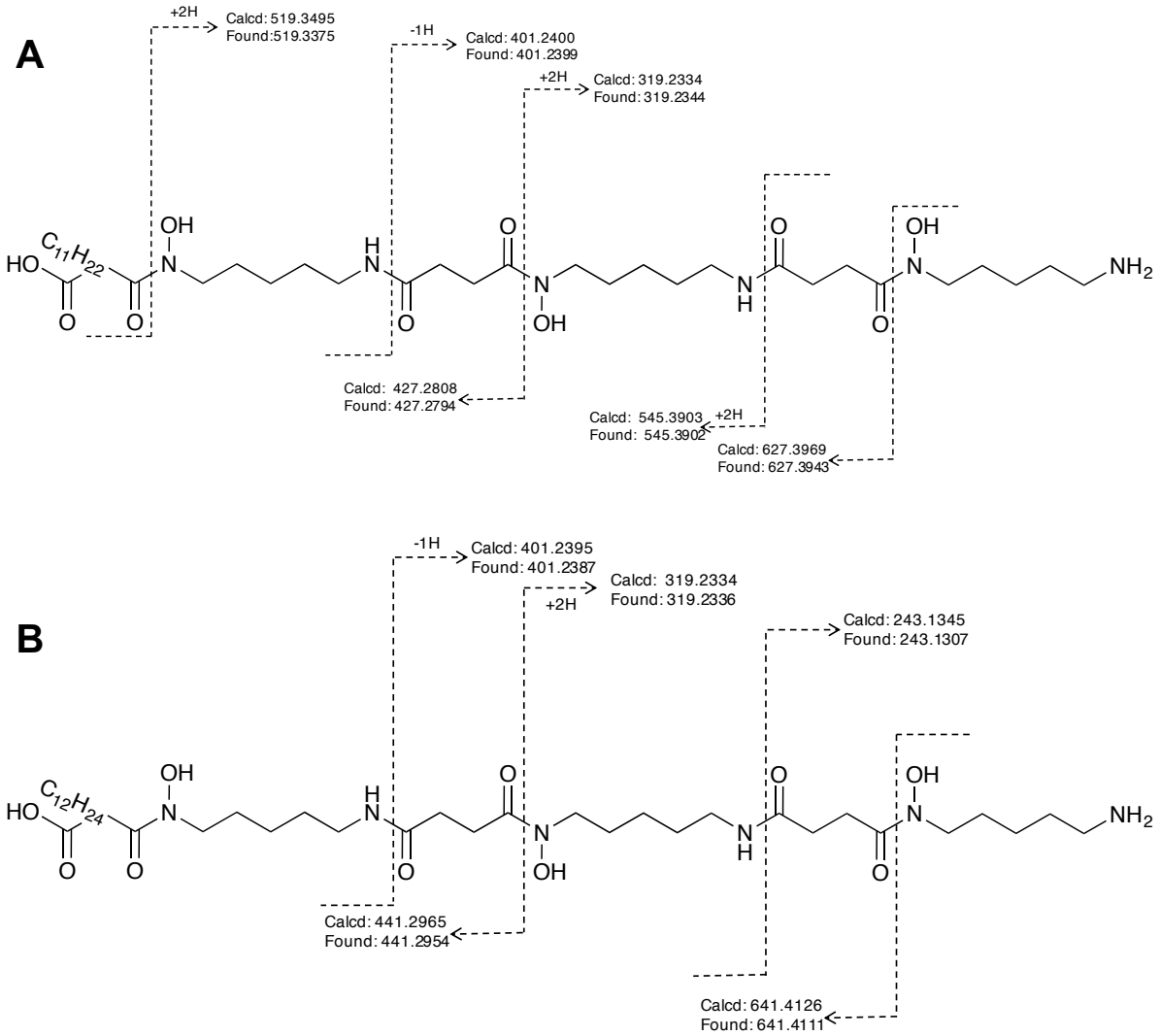

Figure 6. Dicarboxylic acid analogues produced under coculture conditions, (A) Dodecandioic DFO-B and (B) Tridecandioic DFO-B. MS/MS spectra can be found in supplementary data (Figures S26 and S28, respectively).

565